Development of a High-Torque, Low-Cost Electric Bicycle with a Drivetrain Based on the Pinion-and-Pulley System

Davin Tjandra
Department of Mechanical Engineering, Universitas Indonesia, Depok, Indonesia
davin02@ui.ac.id

Muhammad Ilman Mughni
Department of Mechanical Engineering, Universitas Indonesia, Depok, Indonesia
muhammad.ilman02@ui.ac.id

Kevin Dristiani Dani
Department of Mechanical Engineering, Universitas Indonesia, Depok, Indonesia
kevin.dristian@ui.ac.id

A. Ebriel Lianto
Department of Mechanical Engineering, Universitas Indonesia, Depok, Indonesia
a.ebriel@ui.ac.id

Radon Dhelika
Department of Mechanical Engineering, Universitas Indonesia, Depok, Indonesia
radon@eng.ui.ac.id (corresponding author)

Received: 14 April 2025 | Revised: 20 May 2025, 25 May 2025, and 8 June 2025 | Accepted: 9 June 2025

 DOI: https://doi.org/10.48084/etasr.11472

ABSTRACT

The urban mobility is rapidly changing with electric bicycles (e-bikes) becoming the main solution to traffic congestion and air pollution. E-bikes combine electrical components with the design of traditional bicycles, offering an effortless ride with the option of pedaling manually. This study presents an e-bike design with a pinion-and-pulley drivetrain system that aims to optimize the torque and weight distribution. The research focuses on developing, testing, and openly sharing a prototype of a converted e-bike with this system. After driving tests, the estimated maximum distance for the prototype was 30.08 km on a single charge at full throttle.

Keywords-high torque; electric bike; electric bike conversion; pinion-pulley

I. INTRODUCTION

The urban mobility landscape is going through a period of substantial transformation. Using different types of transportation vehicles has increased significantly, with electric vehicles being one of them [1–5]. E-bikes constitute a solution to the urban traffic congestion and air pollution while providing health benefits. The former are bicycles that have electrical components, enabling users to travel effortlessly through various terrains while retaining the traditional bicycle's advantages, such as the manual pedaling capability when the electrical system fails or runs out of energy [6]. The e-bike market uses the hub-drive designs in which the motor is integrated into the wheel hub, as shown in Figure 1 [7-12]. The design is very simple, cost-effective, and has low maintenance requirements, rendering it ideal for urban transportation. However, its efficiency is reduced by the absence of gears and lower torque, which may result in uneven weight distribution [6, 7]. An alternative design is the mid-drive configuration, which mechanically connects the electric motor to the bicycle's pedals, thus providing greater torque, which is better for the difficult terrain, but has a higher cost [9-11]. This study introduces a novel design that differs from the conventional hub-drive model by using a pinion-and-pulley system [13-15]. The proposed design integrates the rear wheel with the motor via a timing belt, enhancing the torque through an optimized pinion-to-pulley ratio. This setup improves the weight

distribution by avoiding the motor installation in the hub and allowing the use of smaller motors, which offer comparable torque to other e-bikes, supporting the growing demand for e-bike conversion kits. The project includes the design phase, manufacturing and assembly processes, and testing in order to validate the prototype's performance and feasibility.

II. LITERATURE REVIEW

The research interest in e-bikes has increased, followed by their classification, which is typically based on the position of the motor. In hub-drive systems, the motor is integrated into a wheel hub, as depicted in Figure 1, while in mid-drive systems the motor is mounted near the crank or pedals to drive the bicycle's chain or gearbox. It is evident that each architecture offers a unique set of performance characteristics.

Fig. 1. Typical electric bicycle with a hub-drive design.

Hub-drive motors occupy a predominant position in the consumer market, attributable to their simplicity and minimal maintenance requirements [16]. The integration of the motor wheel within the hub drives eliminates the need for chain transmission, resulting in a mechanically straightforward design that is cost effective. However, due to the absence of multi-speed gearing in most hub drives, the torque output is constrained at low speeds, resulting in diminished hill-climbing efficiency. The additional mass in the wheel has the tendency to worsen the weight distribution and handling. Mid-drive designs resolve these issues by channeling the power through the bicycle's conventional drivetrain. A mid-drive motor is advantageous when operated with gear reduction, as this configuration enables higher torque at the wheel and ensures more efficient operation across varied speeds and terrains [16]. Authors in [17] reported that an identical e-bike consumed approximately 18% less energy on steep grades with a mid-drive motor compared to a hub motor. This reduction in energy consumption can be attributed to the motor operating in a more efficient RPM range via the bike's gears. Mid-drive systems have been shown to centralize the mass on the frame, thus improving the balance. This approach, however, comes with a trade-off, namely an increase in the mechanical complexity and cost. High-performance mid-drive e-bikes are significantly more expensive than hub-driven models, because they weight approximately 22 kg and necessitate robust transmission components to manage the motor's torque, resulting in increased system costs and maintenance requirements [11]. In addition to the conventional hub and mid-drive layouts, alternative drivetrain concepts were examined to combine the strengths of both. Drive systems that use belts or pulleys represent a better approach, because the motor is mounted to the frame and connected to the rear wheel through a timing belt and pulley (or pinion) system. This configuration allows for the multiplication of the torque through an optimized gear ratio, while circumventing the unsprung weight typically associated with a hub motor. Belt-drive systems offer the benefit of quiet, lubrication-free operation, and high transmission efficiency (on the order of 95%–98% in well-aligned conditions) compared to chains [11]. There is a consensus that each drivetrain type exhibits inherent trade-offs. Specifically, hub drives are characterized by their simplicity and cost-effectiveness, mid-drives are renowned for their ability to deliver high torque, and emerging belt/pulley systems aim to optimize performance while minimizing the maintenance requirements.

III. METHODOLOGY

A. Mechanical Design

The proposed design diverges from the conventional hub motor used in e-bikes, relying on a pinion-and-pulley system integrated with a Brushless DC (BLDC) motor, as portrayed in Figure 2. The drivetrain consists of a pinion, a pulley, and a timing belt. The pinion plays a critical role in the transmission of the torque from the motor shaft to the timing belt, while the timing belt serves as the medium for the transmission of the motor torque from the pinion to the pulley [13, 14]. Subsequently, the pulley affixed to the rear wheel transfers the motor torque to the bicycle wheel. The dimensions of the pulley and pinion are based on the selected timing belt, which is determined by the torque and power transmission requirements for the intended use of the bicycle. The selection of the appropriate pinion and pulley ratio is based on a multifaceted analysis that includes various parameters, such as maximum incline, acceleration, user weight, and mass distribution. It is estimated that the required Total Tractive Effort (TTE) to accelerate a 70-kg rider and a 28-kg bicycle at 2 m/s^2 on a 5-degree incline is approximately 317 N. However, the actual torque delivered by the drivetrain is determined by the gear ratio and motor torque. The ratio of the pinion (20T) to the pulley (175T) results in a gear ratio of 8.75. Given the motor's maximum torque of 8 Nm, the drivetrain torque is calculated as:

$$\tau = \text{Motor torque} \times \text{Gear ratio} = 70 \text{ Nm} \quad (1)$$

Conversely, based on TTE, a transmission efficiency of approximately 0.85 and a wheel radius of 0.2921 m, the obtained torque is 78.65 Nm. The value of 70 Nm from (1) is slightly below the required 78.65 Nm from the TTE-based estimation, but is still considered acceptable. This is due to the fact that the estimated tractive effort may include conservative assumptions, and efficiency losses may be offset by rolling resistance and terrain variability. In this research, the Genio M572, a 27.5-inch mountain bike, is developed. The mechanical design is composed of two sub-assemblies: the motor assembly and the pulley assembly. The pulley assembly

comprises all components that facilitate the connection between the pulley and the bicycle hub. The motor assembly consists of elements that enable the mounting of the motor on the bicycle frame, as presented in Figure 3.

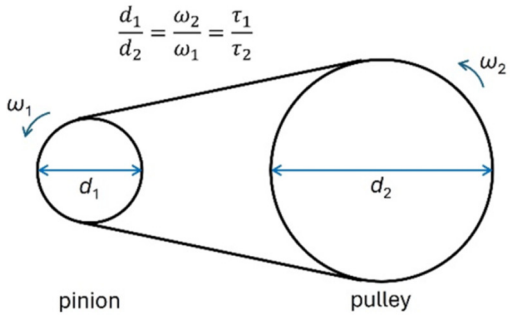

Fig. 2. Illustration of the pinion and pulley system, relating diameters, angular velocities, and torques.

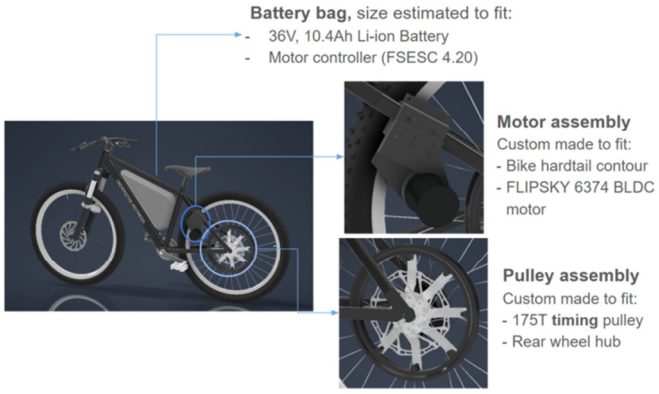

Fig. 3. Placement of the motor assembly and pulley assembly on the bicycle.

As shown in Figure 4, the pulley assembly's design incorporates a timing pulley affixed to the rear tire, with a disc brake serving as a reference point. The timing pulley is linked to the timing pinion mounted on the motor shaft, with both components connected by a timing belt. The high torque of this bicycle is achieved by adjusting the gear ratio between the timing pinion and the timing pulley to 20:170, thereby increasing the torque by 8.5 times. Given that the motor's maximum torque is 8 Nm, the system produces a maximum torque of 68 Nm. This substantial torque capacity enables the bicycle to traverse challenging terrains, including uphill roads, rocky paths, and clay surfaces. Furthermore, as presented in Figure 4, the system uses three plates: two metal (parts 2 and 4 and one plastic (part 6). These plates function to clamp the spokes of the pulley connected to the disc brake on the rear wheel axle, increasing the strength and stability under dynamic loads. The remaining components, parts 1, 3, and 5, respectively, represent the rear tire, the spokes, and the pulley chamfer. Figure 5 displays the design of the motor assembly in an expanded view. The system under consideration consists of a BLDC motor and mounting affixed to the upper portion of the bicycle hardtail via a clamping mechanism. The motor assembly is then adjusted to ensure that the pinion attached to the motor aligns with the timing pulley, ensuring optimal timing belt tension. The attachment of the motor to the mount, and subsequently the motor mount to the bicycle frame, was achieved by using the M4 and M5 bolts. Furthermore, holes were drilled through both the motor mount and the frame to securely attach the connection between the motor and the frame and prevent any shifting due to the tension of the timing belt. The assembly of the primary mounting components was made through the usage of three-dimensional printing methodologies employing Polylactic Acid (PLA) filaments. Following the successful installation of the motor and pulley units, the timing belt was installed to connect these two sub-assemblies.

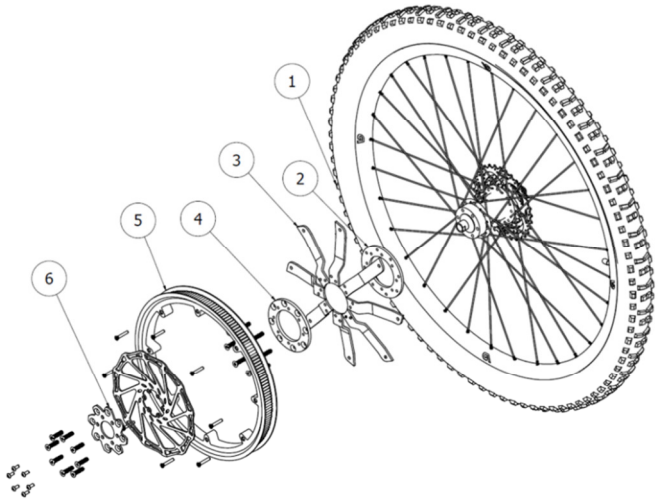

Fig. 4. Expanded view of the pulley assembly.

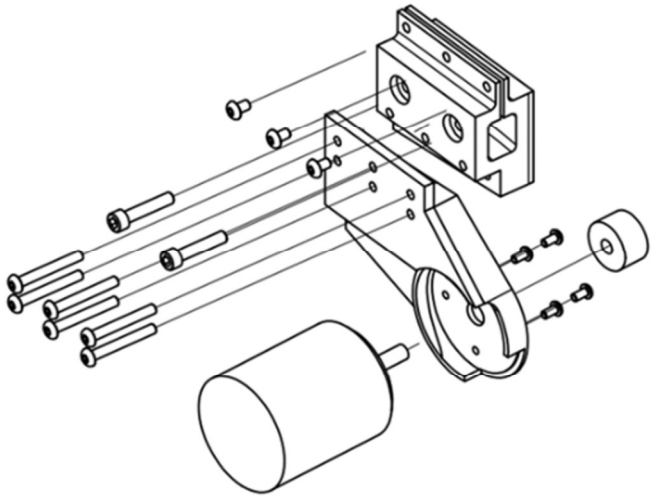

Fig. 5. Expanded view of the motor assembly.

B. Electrical and Electronic Design

The proposed design differs from the hub motor used in conventional e-bikes by using a pinion-and-pulley system integrated with a BLDC motor and the drivetrain includes a pinion, a pulley, and a timing belt [18-20]. Subsequently, the pulley affixed to the rear wheel transmits the motor torque to the bicycle wheel. The components, including the motor,

controller, and battery management system, are selected and calculated with attention to ensure compatibility. The prototype uses a BLDC-type motor due to its high efficiency, high torque, effective cooling characteristics, and low noise pollution. Specifically, the electric motor employed is the FLIPSKY 6374 140 kV, with detailed specifications provided in Table I.

TABLE I. SPECIFICATIONS OF FLIPSKY 6374 BLDC MOTOR

Attribute	Value
Max power	3250 W
Max current	85 A
Max voltage	50.4 V
Max torque	8 Nm
Max RPM	9576 RPM

In order to control the speed of the BLDC motor, an Electronic Speed Controller (ESC) is required, which is responsible for regulating the current supplied from the battery to the motor. It is important that the ESC's maximum current capacity exceeds the motor's maximum current requirement to ensure optimal performance and safety. The specifications for the selected FSESC 6.7 controller are provided in Table II.

TABLE II. SPECIFICATIONS OF FSESC ELECTRONIC SPEED CONTROLLER

Attribute	Value
Current	60 A continuous / 150 A peak
Voltage	8 V - 60 V
BEC	5 V - 1.5 A

The schematic of the electrical system is shown in Figure 6. The electric bicycle is powered by a lithium-ion battery, which has been selected for its safety and durability in electric vehicles. The battery cells are 3.6 V and 2600 mAh, arranged in a 10S4P configuration, resulting in a total capacity of 36V and 10,400 mAh. The vehicle's substantial capacity is indicative of its longevity and its ability to effectively navigate uphill terrain. The battery is connected to the FSESC controller, with the negative terminal connected to V- and the positive terminal connected to V+ on both the controller and the throttle. The input signal originates from the throttle and is transmitted to the controller, which adjusts the BLDC motor's output speed. Prior to the output signal's transmission from the controller to the BLDC motor, it undergoes a series of assessments through the hall sensor. The hall sensor generates a proportional voltage, enabling the BLDC motor to rotate in accordance with the data transmitted by the FSESC controller [21, 22]. The Uniform Resource Locators (URLs) provide three key elements: firstly, an open-source file design that can be modified; secondly, an open-source file to program electrical devices that can be modified with FSESC software; and thirdly, step-by-step building instructions.

IV. RESULTS AND DISCUSSION

After the components were assembled, including the pulley system and the motor system, as illustrated in Figure 7, user testing and evaluation of the e-bike prototype were conducted, including driving tests, battery performance assessments, and maximum range evaluations to validate its functionality and efficiency.

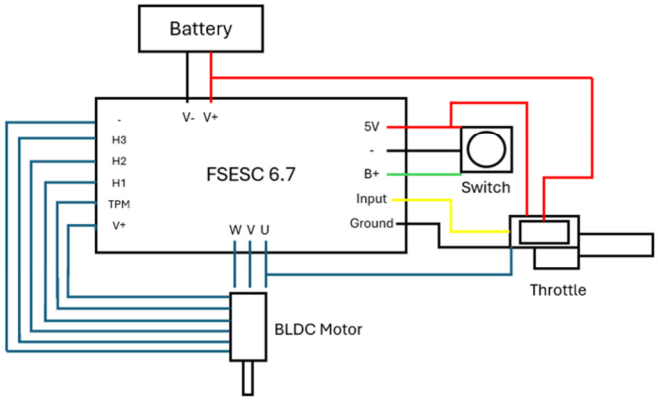

Fig. 6. Schematic of the electrical system.

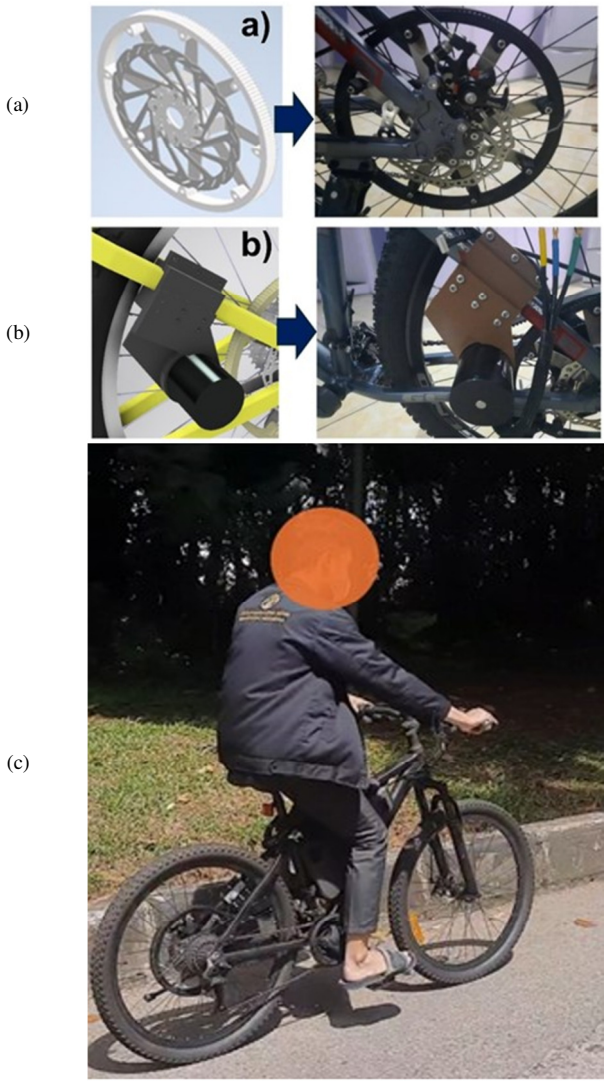

Fig. 7. (a) Manufactured and assembled pulley assembly, (b) manufactured and assembled motor mount assembly, and (c) photo of the developed prototype e-bike on a driving test in Universitas Indonesia.

A. Driving Test

Driving tests were conducted to evaluate the construction of the e-bike conversion. The objective of these tests was to ascertain that the bicycle met the requisite safety standards, which were in accordance with the Indonesian standard SNI 1049:2008 [23], equivalent to EN 15194:2017. During the course of the tests, the maneuverability and reliability of the added components were assessed, revealing no safety concerns. Preliminary visual inspections indicated that all components remained undamaged and did not require readjustment. The bicycle demonstrated its functionality by successfully navigating various terrains and scenarios, including one-handed operation for signaling to other vehicles. A brief video illustrating the e-bike driving examination at the Universitas Indonesia campus is accessible online [24].

B. Battery Performance and Maximum Range

A test drive was conducted on the Universitas Indonesia campus, which included a variety of terrains, namely uphill, downhill, and sharp turns. The cyclist, a 57 kg male, used solely the throttle for acceleration, without pedaling. The data were collected using the Strava mobile application, which was kept open on a mobile phone carried by the cyclist during the test. It is hypothesized that the collected data, when assessed in light of the established parameters, will demonstrate a high degree of correspondence to the real-world conditions under which the prototype will be used. Subsequently, these data were analyzed to predict the maximum distance and duration the prototype can travel before the battery is depleted. Prior to the commencement of the test drive, the battery voltage was recorded at 41.3 V, while the post-test drive reading was recorded at 40.8 V. Consequently, the voltage drop during the test was 0.5 V. The prototype completed the course with an average speed of 14.3 km/h, covering a distance of 1.68 km in 7 min and 4 s. The battery in question has an upper voltage limit of 42 V and a lower limit of 34 V. The percentage of the battery consumption can be calculated using:

$$\%\,Battery\ consumption = \frac{V_1 - V_2}{\Delta V} = \frac{V_1 - V_2}{V_{upper} - V_{lower}} \quad (2)$$

where V_1 and V_2 represent the voltage before use and after use, respectively, and V_{upper} and V_{lower} are the upper voltage limit and lower voltage limit, respectively. Inserting the obtained values, the battery's consumption to cover a distance of 1.68 km is determined to be 6.25%. Subsequently, the theoretical maximum distance can be calculated from the obtained values by comparing them to the battery in full capacity (100%), as:

$$Maximum\ distance = \frac{\%\,Battery\ consumption}{\%\,Battery\ full\ capacity} \times d \quad (3)$$

where d is the distance traveled. Using the experimental data from the test drive, the theoretical maximum distance is 26.88 km. It is important to note that the maximum distance is affected by several factors, including the driving terrain (offroad, city road, uphill, downhill), the cyclist's weight, average speed, and frequency of braking. Furthermore, the voltage drop in a lithium-ion battery is non-linear. The voltage drop becomes significant below 34 V, so 34 V was designated as the lower limit for the battery. To ensure the accuracy of the maximum battery capacity prediction, the prototype was subjected to driving tests under real-world conditions, including traversing rough terrain, ascending inclines, navigating asphalt surfaces, and traversing off-road paths. A randomly selected participant, a 78-kg male, used the bicycle primarily for daily commuting from the student housing to the campus over a period of five days, and recorded the results in a logbook. The data are presented in Table III, which shows that a distance of 17.3 km led to a voltage decline from 42 V to 37.4 V, indicative of a battery consumption of 57.5%. The maximum range with a full charge was determined to be 30.08 km, closely aligning with the prediction.

TABLE III. COMPARISON WITH OTHER COMMERCIALLY-AVAILABLE BIKES

E-bike	E-bike prototype (this research)	Selis Tornado	Selis Roadmaster
Maximum distance	30.08 km (full throttle)	60-80 km (pedal assist) full-throttle mode data not available	35 km (full throttle)
Battery capacity	10.4 Ah	10.4 Ah	10 Ah
Max speed	> 25 km/h	>25 km/h	25 km/h
Cost	$ 621.47	$ 1342	$ 1074

C. Component Reliability

The force necessary to accelerate a 70-kg rider on a level surface at a rate of 2 m/s² is 196 N. Therefore, the torque required of the rear wheel is 57.25 Nm:

$$Belt\ Tension = \frac{\tau}{Pulley\ Radius} \times FOS \quad (4)$$

where τ is the torque and FOS is the Factor of Safety. According to (4), the belt tension is measured at 613.8 N, which is the minimum force that the motor mount and the spokes must be able to withstand. Assuming that the force is equally distributed among the eight spokes, it can be calculated that each spoke must be capable of handling a force of 76.67 N. To verify the mechanical integrity of the spokes and motor mount under this load, stress simulations were conducted using Autodesk Inventor, as presented in Figures 8 and 9. Aluminum 6061, a material frequently used in the fabrication of bicycle components, possesses an approximate yield strength of ~276 MPa. The result of this study, 113.5 MPa, is 41% below this limit, indicating a high safety margin. In a similar vein, while PLA is not generally employed in long-term load-bearing applications, the stress value of our design (8.53 MPa) remains well below the PLA yield strength (~26 MPa), thereby providing an initial prototype solution. Consequently, the components installed on the prototype are suitable for their intended use. However, while PLA is sufficient for preliminary testing, it may not be ideal for long-term durability under cyclic mechanical loads and environmental exposure, such as heat and moisture. Subsequent prototypes should consider replacing the PLA mount with a more robust material, such as aluminum or carbon fiber-reinforced polymer, to enhance the structural reliability and longevity.

D. Comparison with other Commercially Available E-bikes

The estimated maximum distance of the prototype is 30.08 km on a single charge (full throttle), which is within a reasonable range when compared to other products. A

comparison of the prototype with Selis Tornado and Selis Roadmaster models reveals that it exhibits competitive performance despite its lower cost. It is noteworthy that while Selis Tornado claims a range of 60–80 km under pedal assist, its full-throttle performance remains unreported. The prototype achieved a range of 30.08 km in full-throttle mode, which is comparable to the Selis Roadmaster's range of 35 km. Moreover, the prototype offers a cost-effective alternative, with the converter kit costing approximately $511 and providing a versatile option for the bicycle frame (the frame of Genio M572 used in this study costs around $110.47). A thorough cost analysis will include all components from design to manufacturing. This preliminary comparison offers an initial overview of the potential of the proposed e-bike design featuring a pinion-and-pulley drivetrain system.

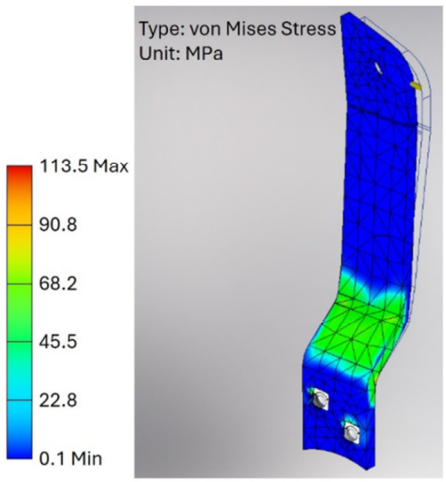

Fig. 8. Von Mises stress analysis of the spoke under loading conditions. The maximum stress occurs near the spoke-pulley interface and is indicated by the red region in the color bar, with a peak value of 113.5 MPa.

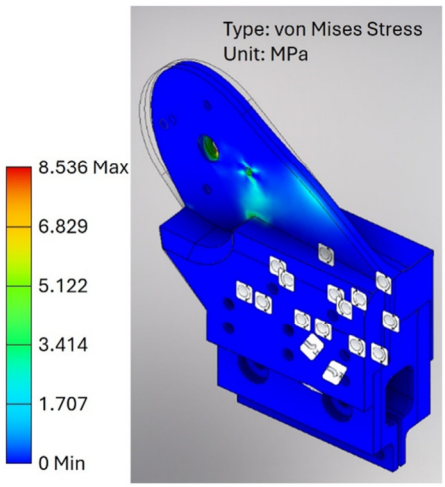

Fig. 9. Von Mises stress analysis of the motor mount under tension from the timing belt. The maximum stress is indicated by the red region in the color bar, with a peak value of 8.536 MPa.

V. CONCLUSIONS

The Electric bike (e-bike) prototype equipped with a pinion-and-pulley drivetrain system exhibited successful functionality, with the design offering a viable alternative to traditional hub-drive and mid-drive designs, potentially leading to more cost-effective and high-performance e-bikes in the future. This innovation has the potential to contribute to the reduction of urban congestion and pollution, thereby fostering more sustainable cities. The prototype was subjected to a rigorous testing process, including driving assessments and battery performance evaluations, yielding encouraging results. The maneuverability and reliability of the added components were assessed, and no safety concerns were revealed. These findings were confirmed through visual inspection, mathematical analysis, and simulations. The bicycle demonstrated a smooth operation in a variety of scenarios. The estimated maximum distance of the prototype is 30.08 km on a single charge with full throttle, which is competitive with other commercially available e-bikes in Indonesia. In the future, improvements may be made in several areas. The assembly may be redesigned to be as adaptable as possible for compatibility with most bicycles. The manufacturing processes may be evaluated, and a thorough analysis of the design for manufacturing and the design for assembly may be performed to enhance efficiency.

ACKNOWLEDGMENT

This project is partially funded by the Tanoto Student Research Award.

REFERENCES

[1] A. Bawa and M. N. Nwohu, "Investigating the Penetration Rate of Electric Vehicle in Developing Countries: Nigeria as A Case Study," in *International MultiConference of Engineers and Computer Scientists*, Hong Kong, China, Jul. 2023.

[2] K. Unni and S. Thale, "Energy Consumption Analysis for the Prediction of Battery Residual Energy in Electric Vehicles," *Engineering, Technology & Applied Science Research*, vol. 13, no. 3, pp. 11011–11019, Jun. 2023, https://doi.org/10.48084/etasr.5868.

[3] A. Khadhraoui, T. Selmi, and A. Cherif, "Energy Management of a Hybrid Electric Vehicle," *Engineering, Technology & Applied Science Research*, vol. 12, no. 4, pp. 8916–8921, Aug. 2022, https://doi.org/10.48084/etasr.5058.

[4] D. D. Trung, D. H. Tien, and N. H. Son, "Decısıon makıng for car selectıon ın Vıetnam," *EUREKA: Physics and Engineering*, no. 6, pp. 139–150, Nov. 2022, https://doi.org/10.21303/2461-4262.2022.002505.

[5] D. D. Trung, B. Dudić, N. C. Bao, H. Xuan Thinh, D. Van Duc, and A. Ašonja, "Applying Probability Method for Battery Electric Vehicle Selection," in *2025 24th International Symposium INFOTEH-JAHORINA (INFOTEH)*, East Sarajevo, Bosnia and Herzegovina, Mar. 2025, pp. 1–5, https://doi.org/10.1109/INFOTEH64129.2025.10959268.

[6] E. Salmeron-Manzano and F. Manzano-Agugliaro, "The Electric Bicycle: Worldwide Research Trends," *Energies*, vol. 11, no. 7, Jul. 2018, Art. no. 1894, https://doi.org/10.3390/en11071894.

[7] S. K. Chawrasia, A. Das, C. K. Chanda, and S. Banerjee, "Design, analysis and comparative study of Hub motor for an electric bike," in *Michael Faraday IET International Summit 2020 (MFIIS 2020)*, Online Conference, Jul. 2020, vol. 2020, pp. 242–247, https://doi.org/10.1049/icp.2021.1179.

[8] S. K. Chawrasia, A. Das, and C. Kumar Chanda, "Design and Analysis of Electric bike Hub-Motor using Motor-CAD," in *2020 3rd International Conference on Energy, Power and Environment: Towards*

Clean Energy Technologies, Shillong, Meghalaya, India, Mar. 2021, pp. 1–6, https://doi.org/10.1109/ICEPE50861.2021.9404475.

[9] N. B. Hung and O. Lim, "A review of history, development, design and research of electric bicycles," *Applied Energy*, vol. 260, Feb. 2020, Art. no. 114323, https://doi.org/10.1016/j.apenergy.2019.114323.

[10] A. Z. Aliyadin, A. Purwadi, and S. Hidayat, "Performance Analysis and Design of 250 Watt Outer Rotor BLDC Motor for Urban Electric Bicycles," in *7th International Conference on Electric Vehicular Technology (ICEVT)*, Bali, Indonesia, Sep. 2022, pp. 195–199, https://doi.org/10.1109/ICEVT55516.2022.9925011.

[11] M. V. Terzić and D. S. Mihić, "Switched Reluctance Motor Design for a Mid-Drive E-Bike Application," *Machines*, vol. 10, no. 8, Aug. 2022, Art. no. 642, https://doi.org/10.3390/machines10080642.

[12] T. Van Huy *et al.*, "Multi-criteria decision-making for electric bicycle selection," *Advanced Engineering Letters*, vol. 1, no. 4, pp. 126–135, 2022, https://doi.org/10.46793/adeletters.2022.1.4.2.

[13] Tom Stanton, *Electric bike 4.0 - Pulley*,: https://www.youtube.com/watch?v=cQhZSc0dhjc.

[14] P. Li and Q. TU, "Middle electric motor drive unit for electric bicycle," US8205705B2, Jun. 26, 2012.

[15] F. Roos and J. Wikander, "The influence of gear ratio on performance of electromechanical servo systems," *IFAC Proceedings Volumes*, vol. 39, no. 16, pp. 884–889, Jan. 2006, https://doi.org/10.3182/20060912-3-DE-2911.00152.

[16] S.-P. Zhang and T.-O. Tak, "Efficiency Evaluation of Electric Bicycle Power Transmission Systems," *Sustainability*, vol. 13, no. 19, Jan. 2021, Art. no. 10988, https://doi.org/10.3390/su131910988.

[17] I. Arango, A. Godoy, and C. Lopez, "E-bikes for steep roads: mid drive and hub drive motor efficiency comparison," *International Journal of Vehicle Systems Modelling and Testing*, vol. 13, no. 1, 2018, Art. no. 44, https://doi.org/10.1504/IJVSMT.2018.094587.

[18] S. Chauhan, "Motor Torque Calculations For Electric Vehicle," *International Journal of Scientific & Technology Research*, vol. 4, no. 08, pp. 126–127, 2015.

[19] R. Perneder and I. Osborne, *Handbook Timing Belts: Principles, Calculations, Applications*, 1st ed. Berlin, Heidelberg: Springer, 2012.

[20] E. Avila, "Design of a tricycle chassis using computer-aided design and finite element analysis," Ph.D. dissertation, Massachusetts Institute of Technology, Cambridge, MA, USA, 2014.

[21] Davin, "High Torque Electric Conversion Mountain Bike - Pulley Mount," Dec. 2022, https://doi.org/10.5281/zenodo.7154190.

[22] Davin, "High Torque Electric Conversion Mountain Bike - Motor Mount," Dec. 2022, https://doi.org/10.5281/zenodo.7147860.

[23] *SNI No. 1049:2008 Bicycles – Safety requirements*. Indonesia: The Standarization Council of Indonesia, 2008.

[24] *High Torque Bike Conversion (HTBC)*. 2023, https://www.youtube.com/watch?v=AIX3c1cFIfY.